IEEE Access
Multidisciplinary | Rapid Review | Open Access Journal

Received July 24, 2021, accepted July 30, 2021, date of publication August 4, 2021, date of current version August 13, 2021.

Digital Object Identifier 10.1109/ACCESS.2021.3102296

Day-Ahead Scheduling of Power System With Short-Circuit Current Constraints Considering Transmission Switching and Wind Generation

HAOCHENG HUA[1], TIANQI LIU[1], (Senior Member, IEEE), CHUAN HE[1], (Member, IEEE), LU NAN[1], (Member, IEEE), HONG ZENG[2], XIAOTONG HU[3], AND BIN CHE[4]

[1]College of Electrical Engineering, Sichuan University, Chengdu, Sichuan 610065, China
[2]Tianfu Power Supply Company, State Grid Sichuan Electrical Power Company, Chengdu, Sichuan 610041, China
[3]State Grid Sichuan Electrical Power Company, Chengdu, Sichuan 610041, China
[4]Economic and Technological Research Institute, State Grid Ningxia Electric Power Company Ltd., Yinchuan 750004, China

Corresponding author: Lu Nan (lnan@scu.edu.cn)

This work was supported by Sichuan Science and Technology Program under Grant 2021YFH0029.

ABSTRACT The expansion of the power network and integration of wind farms pose challenges in the short-circuit current (SCC) problem. Transmission switching performs better in both flexibility and effectiveness compared with other SCC restriction measures, while the power grid security would be threatened as the number of switched-off-lines increases. This paper proposes a day-ahead scheduling model considering commitment of units and N-1 criterion, to avoid the excessive SCC problem caused by wind farms integration. Specially, the SCC calculation model of the grid-connected wind farms is put forward to aggregate wind farms and calculate SCC. A novel SCC formulation considering transmission switching, commitment of units as well as wind farms integration is deduced and converted to SCC constraints. The SCC constrained mixed-integer linear programming (MILP) based day-ahead scheduling model is proposed, which minimizes system operation cost and transmission switching cost. In addition, the N-1 security requirement is considered in the proposed day-ahead scheduling model to ensure system security by avoiding switching off too many lines. Numerical results of a modified IEEE 30-bus system with two wind farms illustrate effectiveness of the proposed model.

INDEX TERMS Short-circuit current, wind farm integration, transmission switching, day-ahead scheduling, mixed-integer linear programming.

NOMENCLATURE

Major symbols and notations used throughout the paper are defined below, while others are defined following their first appearances as needed.

Indices:

l, g, w	Indices of lines, thermal generating units and wind farms.
t, n, c, d	Indices of hours, buses, contingency statuses and loads.

Variables:

c_g	Marginal operation cost of unit g.
c_l	Operation cost of switching line l.
$I_{g,t}, I_{w,t}$	Commitment indicators of unit g/wind farm w at hour t.
$s^c_{l,t}$	Binary variable represents operation status of line l at hour t, which is equal to 1 if line l is tripped out in contingency, being 0 otherwise.
$SU_{g,t}, SD_{g,t}$	The startup/shutdown cost of unit g at hour t.
$X^{\text{on}}_{g,t}, X^{\text{off}}_{g,t}$	Uptime/downtime counter of unit g at hour t.
μ_l, π_g, λ_w	Binary operation variables which are equal to 0 if line l/unit g/wind farm w is in service, being 1 otherwise.
$\theta_{n,t}, P_{g,t}, P_{w,t}$	Angle of bus n, generation of unit g and dispatch of wind farm w at hour t.

Constants:

$D_{d,t}$	Demand of load d at hour t.
L, G, W, N	The number of lines, units, wind farms and buses.

The associate editor coordinating the review of this manuscript and approving it for publication was Arturo Conde.

J_t	Allowable number of switched-off lines at hour t.
I_n^{limit}	Threshold value of SCC at investigated bus n.
M	Large enough number.
$P_{w,t}^f$	Wind power forecast of wind farm w at hour t.
$P_l^{\min}$, $P_l^{\max}$	Minimum/maximum power flow of line l.
$P_g^{\min}$, $P_g^{\max}$	Minimum/maximum output of unit g.
su_g, sd_g	Startup/shutdown fuel consumption of unit g.
T_g^{on}, T_g^{off}	Uptime/downtime limit of unit g.
UR_g, DR_g	Up/ down ramping limit of unit g.
x_g, x_w^g	Subtransient reactance of unit g/wind farm equivalent WTG.
z_w^l	Equivalent impedance of grid-connected wind farm w.
y_l, z_l	Admittance/impedance of line l.
z_{nn}^0	Original nodal self-impedance of bus n with all lines, wind farms and units in service.
$\theta^{\min}$, $\theta^{\max}$	Minimum/maximum value of bus angles.
Functions and Sets:	
$F_g(\cdot)$	Heat rate curve of unit g.
$s(l)$, $r(l)$	Sending bus and receiving bus of line l.
Ω_{L}, Ω_{G}, Ω_{W}	Set of lines, units, wind farms.
Ω_{N}, Ω_{S}	Set of buses and investigated buses with SCC constraints.
Arrays and matrixes:	
Y_0, Z_0	Original admittance/impedance matrix with all lines, wind farms and units in service.

I. INTRODUCTION

A. MITIVATION AND INCITEMENT

The enhancement of power grid network topology worsens the excessive short-circuit current (SCC) problem, especially with the intensified integration of wind farms [1], [2]. Transmission switching is carried out to optimize system operation and reduce the SCC level of power grid by changing the network topology, which works well without adding extra electrical equipment and consequently achieving significant savings [3]. However, transmission switching may weaken the system security and the N-1 security may not be ensured when a large number of transmission lines are switched off [4]. Specifically, the startup and shutdown of generators could affect the SCC level. In turn, it is essential to restrict the SCC level of power system considering transmission switching and commitment status of units as well as wind farms integration.

B. LITERATURE REVIEW

Previous research mostly focuses on the stability analysis of grid-connected wind farms, and few studies the impact of wind farms integration on the SCC. To analyze the impact of grid-connected wind farm on SCC, it is crucial to deduce the SCC equivalent model of wind farms. There are two main categories to obtain the SCC equivalent model of wind farms [5]: parameter identification method [6] and wind turbine generators (WTGs) capacity weighting method [7]. The parameter identification method is used to optimize the parameters of the equivalent WTG and consequently improve the identification efficiency [8]. The objective is to minimize the output error before and after the WTG equivalent process. Additionally, clustering algorithm is also used to analyze and cluster the WTG parameters, such as fuzzy clustering algorithm [9] and K-means clustering algorithm [10]. For another method, the parameters of WTG capacity weighting method could be obtained by calculating the weighted average value of WTG parameters. The wind generation of the wind farm is dynamically weighted to obtain the output of its equivalent aggregated WTG [11]. In general, a grid-connected wind farm can be converted to an equivalent WTG and consequently participates in SCC calculation.

To restrict SCC level, optimal transmission switching is presented. It is firstly used as an optimization approach to manage network congestion of the power grid [12] and reduce operation cost [13], decrease generation dispatch cost [14] and ensure network connectedness [15]. Reference [16] validates that power transmission efficiency could be improved via transmission switching. Transmission switching plays an essential rule in SCC level restriction. In [17], the relationship between SCC and transmission switching is studied and an SCC constrained optimal transmission switching model is proposed. Additionally, researchers are aware of the impact of transmission switching on system security, and the N-1 reliability criterion is adopted to ensure system security [18], [19]. Reference [20] adds the N-1 security in the proposed optimal transmission switching model to improve the system security as several lines are switched off. Researchers focus on transmission switching with security-constrained unit commitment models to reduce operation cost and relieve transmission violations in [21] and [22]. In [23], unit commitment scheduling and transmission switching are co-optimized for reserves. Transmission switching and unit commitment are used to relieve congestion with the renewable energy integration in [24].

From another point of view, the SCC restriction result of transmission switching have certain limitations under the circumstances that switching off too many lines. The system security requirements may not be satisfied because of the switching process. It is noted that the SCC level is also affected by starting up and shutting down the selected units. Practically, the system SCC level is annually checked under the assumption that all units are in service, which might be conservative [25]. And not all units are committed in service all the time in power system operation, which makes SCC

restriction could be achieved through reasonable commitment of units. Hence, SCC restriction measures considering transmission switching and commitment of units are likely to perform better. At present, researches on SCC restriction simultaneously considering transmission switching and unit commitment are limited. Reference [25] proposes a co-optimization model and decomposes the model as a unit commitment master problem and a transmission switching subproblem, which is solved by an iterative algorithm. To the best of authors' knowledge, the SCC restriction model considers both transmission switching and commitment of units with wind farms integration has not been studied in previous research.

C. CONTRIBUTION AND PAPER ORGANIZATION

The paper proposes a mixed-integer linear programming (MILP) based day-ahead scheduling model with SCC constraints, which considers wind farms integration, transmission switching, commitment status of units, and N-1 security requirement. The proposed model minimizes the total cost of system operation and transmission switching. Specially, to ensure the system security, N-1 security criterion is adopted to the proposed day-ahead scheduling model. The major contribution of the paper can be summarized as:

1) The grid-connected wind farms equivalent model is constructed via the single-machine equivalent model. The grid-connected wind farms are aggregated and embedded into the SCC calculation process. Then a novel analytical formulation of SCC considering transmission switching, commitment of units and integration of wind farms is put forward, which is further linearized and converted into SCC constraints to improve computational efficiency and directly participate in the model solving.
2) A day-ahead scheduling model with SCC constraints considering transmission switching and commitment of units as well as N-1 reliability criterion is proposed. The proposed model could keep the benefits of flexibility and cost-efficiency while maintaining system security. To solve the proposed model, an iterative procedure is designed to check N-1 security and compensate for the errors of SCC linearization.

The rest of the paper is organized as follows. Section II discusses the SCC equivalent model of the grid-connected wind farms. The SCC formulation considering transmission switching and commitment of units is introduced in section III. Section IV presents the proposed day-ahead scheduling model and the N-1 security iterative procedure. Several case studies verifying the effectiveness of the proposed model are given in Section V. Finally, the paper is concluded in section VI.

II. THE SCC EQUIVALENT MODEL OF GRID-CONNECTED WIND FARM

To analyze the impact of wind farms integration on SCC level, the single-machine equivalent model of wind farms is introduced in Section II.A. And Section II.B discusses the SCC calculation model based on the wind farm equivalent model and grid-connected wind farm topology.

A. THE EQUIVALENT MODEL OF GRID-CONNECTED WIND FARM

A typical wind farm with several WTGs is shown in Fig. 1. The WTGs of the same type are firstly connected to the branches (e.g., branch 1), and then all branches are merged to bus A. Active power of WTGs is finally delivered to the main grid via branch A-B.

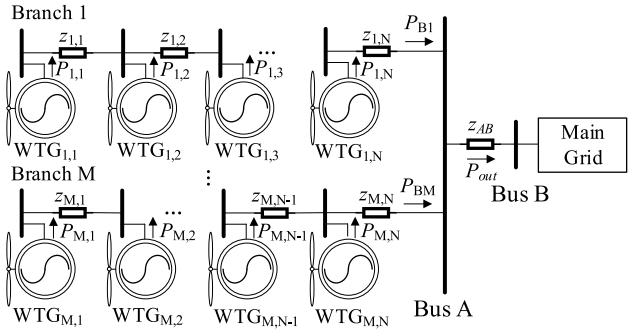

FIGURE 1. Configuration of a grid-connected wind farm.

The single-machine equivalent method [26] is widely used according to the wind farm modeling guidelines from IEC (international electrotechnical commission) and WECC (western electricity coordinating council). A certain number of WTGs of the same type working at similar operation conditions in a wind farm could be equivalently converted to a new aggregated WTG [27]. The capacity of the newly aggregated WTG is equal to the total capacity of all the equivalent WTGs in the wind farm. An equivalent impedance is used to represent the power loss within the wind farm.

Consequently, a wind farm could be converted to a newly aggregated WTG with larger capacity and equivalent impedance. It is noteworthy that the generation output and power loss of the wind farm before and after the aggregation process should be same.

If the WTGs in Fig. 1 are of different types, while the WTGs connecting on the one branch are of the same types, each branch with its WTGs could form a new wind farm subsystem and the multi-machine equivalent model could be obtained, as is shown in Fig. 2(a). Furthermore, if the WTGs in all the subsystems are of the same type, the wind farm could be equivalent to a single-machine equivalent model as in Fig. 2(b).

As shown in Fig. 2(b), the whole wind farm is replaced by a newly equivalent WTG, which is WTG_{eq}. The interconnection, internal loss, and impedance of branch A-B are equivalently transformed to impedance z_w^l. The equivalent system WTG_{eq} is finally connected to the main grid via bus B.

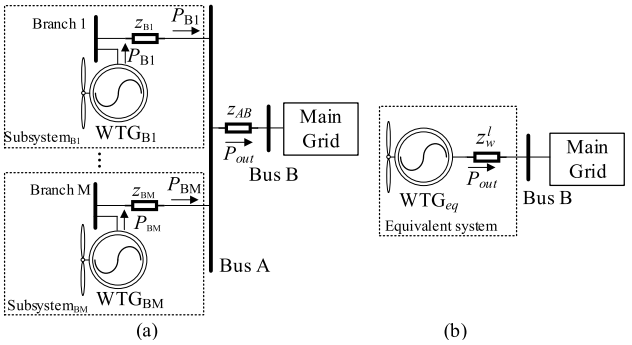

FIGURE 2. Configuration of the equivalent model of the grid-connected wind farm, (a) multi-machine equivalent model with different types of WTGs, (b) single-machine equivalent model with the same type of WTGs.

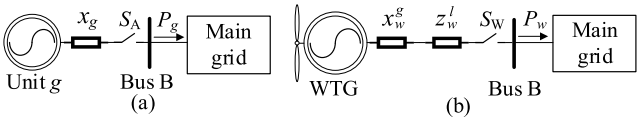

FIGURE 3. SCC calculation model, (a) thermal generating unit, (b) wind farm.

B. THE SCC CALCULATION MODEL OF GRID-CONNECTED WIND FARM

To analyze the impact of WTGs on SCC, the impact of thermal generating units is firstly deduced. The SCC calculation model of thermal generating units is shown in Fig. 3(a). In Fig. 3(a), when switchgear S_A is closed, unit g is in service. The subtransient reactance x_g connecting to the network could increase the system's SCC level, especially the SCC level of the buses around thermal generating units.

Based on the equivalent model of wind farm in Fig. 2(b), the SCC calculation model is profiled in Fig. 3(b). Switchgear S_W determines the operation status of the equivalent WTG, while x_w^g and z_w^l represent subtransient reactance and impedance of the equivalent WTG. It could be concluded that the SCC calculation model of WTGs is similar to the model of thermal generating units. Once S_W is closed, the WTG will be connected to the main grid which will increase the system's SCC level. Therefore, the grid-connected wind farm is aggregated to an equivalent WTG through the single-machine equivalent model, and the equivalent WTG will participate in the SCC calculation via its SCC calculation model.

III. THE SCC FORMULATION

This paper focuses on the SCC problem of high voltage transmission networks where the SCC problem is more severe as compared with distribution network. As a result, only reactance is considered in the proposed SCC formulation model. Because three-phase fault is the most severe one among all types of faults, this paper aims at the three-phase fault and calculate the SCC level of three-phase fault. As three-phase fault is symmetric, only one phase analysis will be conducted in this section. Unless specially noted, the SCC in this paper figures the system's SCC level.

A. BASIC SCC FORMULATION

On account of that the interrupting capacity of the circuit breakers mainly depends on the steady state SCC [28], this paper focuses on the formulation of the steady state SCC, the consideration of transient SCC will be the future research directions. Assume that the voltage of the investigated bus n is U_0 under the normal operation condition, U_n and i_n are the voltage and SCC of bus n after the fault occurs, respectively. The relationship between nodal self-impedance z_{nn}, voltages and SCC at bus n is defined as follows:

$$U_0 = U_n + z_{nn} \cdot i_n \tag{1}$$

After the fault occurs, the voltage of the failed bus changes to 0, that is, U_n becomes 0 [29]. Therefore, the SCC of bus n could be obtained as follows:

$$i_n = U_0 / z_{nn} \tag{2}$$

Because the value of U_0 is constant, and U_0 is approximately 1.0 per unit [29], it could be concluded that increasing the investigated bus's nodal self-impedance could restrict the SCC level. The nodal self-impedance of bus can be increased through transmission switching or decommitting units. The calculation of nodal self-impedance considering transmission switching, commitment of units and wind farms integration will be deduced in the following section.

B. SELF-IMPEDANCE CALCULATION CONSIDERING SINGLE LINE SWITCHING

Suppose that all lines, units and wind farms are in service before taking any SCC restriction measures [17]. The admittance matrix Y_l considering a single switchable line l is calculated as follows:

$$Y_l = Y_0 + E_l(-\mu_l \cdot y_l)E_l^{\mathrm{T}}, l \in \Omega_{\mathrm{L}} \tag{3}$$

where $E_l = [0, \ldots, 1, \ldots, -1, \ldots, 0]^{\mathrm{T}}$ is an array vector, values 1 and -1 represent the sending and receiving bus of line l, respectively.

According to the matrix inverse lemma [30], impedance matrix Z_l can be obtained by inversing the admittance matrix Y_l, as shown in (4)-(5).

$$Z_l = Y_l^{-1} = Z_0 - Z_0 E_l a_l^{-1} E_l^{\mathrm{T}} Z_0 \tag{4}$$

$$a_l = (-\mu_l \cdot y_l)^{-1} + E_l Z_0 E_l^{\mathrm{T}} \tag{5}$$

Nodal self-impedance z_{nn}^l of bus n with line l switched off is derived as follows:

$$z_{nn}^l = D_n^{\mathrm{T}} Z_l D_n = z_{nn}^0 - D_n^{\mathrm{T}}[Z_0 E_l a_l^{-1} E_l^{\mathrm{T}} Z_0] D_n \tag{6}$$

where $D_n = [0, \ldots, 1, \ldots, 0]^{\mathrm{T}}$ represents the location of bus n, and value 1 represents bus n.

Because variable μ_l is binary, the discussion on a_l^{-1} can be divided into two conditions: 1) when line l is switched off, $\mu_l = 1$ and $a_l^{-1} = (-z_l + E_l^{\mathrm{T}} Z_0 E_l)^{-1}$; 2) when line l is in service, $\mu_l = 0$ and $a_l \to \infty$, that is $a_l^{-1} \to 0$. Hence, a_l^{-1} can be rewritten as in (7).

$$a_l^{-1} = (-z_l + E_l^{\mathrm{T}} Z_0 E_l)^{-1} \cdot \mu_l \tag{7}$$

Consequently, the nodal self-impedance z_{nn}^{l} can be calculated according to the original nodal self-impedance z_{nn}^{0}, the compensation impedance Δz_{nn}^{l} and the line status μ_l, as in (8)-(9).

$$\Delta z_{nn}^{l} = D_n^{\mathrm{T}}[-Z_0 E_l(-z_l + E_l^{\mathrm{T}} Z_0 E_l)^{-1} E_l^{\mathrm{T}} Z_0] D_n \quad (8)$$

$$z_{nn}^{l} = z_{nn}^{0} + \mu_l \cdot \Delta z_{nn}^{l}, l \in \Omega_{\mathrm{L}} \quad (9)$$

C. SELF-IMPEDANCE CALCULATION CONSIDERING COMMITMENT OF SINGLE UNIT AND SINGLE WIND FARM

In fact, the impact of unit commitment on SCC mainly depends on the connection of the unit subtransient reactance, which is shown in Fig. 3. When a unit shuts down, its subtransient reactance is simultaneously cut out from the network which will reduce the SCC level of the system, especially the SCC level of the buses around the thermal generating unit.

The admittance matrix with single unit g decommitted is determined as in (10), which is similar to the formulation (3) of transmission switching.

$$Y_g = Y_0 + D_g(-\pi_g \cdot x_g^{-1}) D_g^{\mathrm{T}}, g \in \Omega_{\mathrm{G}} \quad (10)$$

where $D_g = [0, \ldots, 1, \ldots, 0]^{\mathrm{T}}$ represents the location of unit g, value 1 represents the bus with unit g.

Therefore, the nodal self-impedance z_{nn}^{g} of the investigated bus n when unit g is decommitted could be calculated as follows:

$$z_{nn}^{g} = z_{nn}^{0} + \pi_g \cdot \Delta z_{nn}^{g} \quad (11)$$

$$\Delta z_{nn}^{g} = D_n^{\mathrm{T}}[-Z_0 D_g(-x_g + D_g^{\mathrm{T}} Z_0 D_g)^{-1} D_g^{\mathrm{T}} Z_0] D_n \quad (12)$$

where Δz_{nn}^{g} is the compensation impedance when unit g is decommitted.

Similarly, the admittance Y_w and the nodal self-impedance z_{nn}^{w} of bus n as considering the decommitment of wind farm w are shown as follows:

$$Y_w = Y_0 + D_w(-\lambda_w \cdot z_w^{-1}) D_w^{\mathrm{T}}, w \in \Omega_{\mathrm{W}} \quad (13)$$

$$z_w = x_w^{g} + z_w^{l} \quad (14)$$

$$z_{nn}^{w} = z_{nn}^{0} + \lambda_w \cdot \Delta z_{nn}^{w} \quad (15)$$

$$\Delta z_{nn}^{w} = D_n^{\mathrm{T}}[-Z_0 D_w(-z_w + D_w^{\mathrm{T}} Z_0 D_w)^{-1} D_w^{\mathrm{T}} Z_0] D_n \quad (16)$$

where Δz_{nn}^{w} is the compensation impedance considering operation status of the wind farm w; value 1 in $D_w = [0, \ldots, 1, \ldots, 0]^{\mathrm{T}}$ represents the bus with wind farm w; z_w is the total variation impedance reflects operation status of wind farm w.

D. SELF-IMPEDANCE CALCULATION CONSIDERING MULTIPLE LINES SWITCHING, COMMITMENT OF UNITS AND WIND FARMS INTEGRATION

According to (3), (10) and (13), the admittance matrix Y_{all} considering multiple lines switched off, commitment of units and wind farms integration [25] could be quantified as follows:

$$Y_{all} = Y_0 + D_{LGW} M_{LGW} D_{LGW}^{\mathrm{T}} \quad (17)$$

$$D_{LGW} = [E_{l_1}, \ldots, E_{l_{\mathrm{L}}}, D_{g_1}, \ldots, D_{g_{\mathrm{G}}}, D_{w_1}, \ldots, D_{w_{\mathrm{W}}}] \quad (18)$$

$$M_{LGW} = \begin{bmatrix} M_L & & \\ & M_G & \\ & & M_W \end{bmatrix} \quad (19)$$

$$M_L = \mathrm{diag}[-\mu_{l_1} y_{l_1}, \ldots, -\mu_{l_{\mathrm{L}}} y_{l_{\mathrm{L}}}] \quad (20)$$

$$M_G = \mathrm{diag}[-\pi_{g_1} x_{g_1}^{-1}, \ldots, -\pi_{g_{\mathrm{G}}} x_{g_{\mathrm{G}}}^{-1}] \quad (21)$$

$$M_W = \mathrm{diag}[-\lambda_{w_1} z_{w_1}^{-1}, \ldots, -\lambda_{w_{\mathrm{W}}} z_{w_{\mathrm{W}}}^{-1}] \quad (22)$$

where D_{LGW} is the matrix consists of the location vectors of all switchable lines, units and wind farms; M_{LGW} is a diagonal matrix with operation variables representing the statues of transmission lines, thermal generating units and wind farms.

Similarly, the nodal self-impedance z_{nn}^{lgw} of bus n could be deduced as follows:

$$z_{nn}^{lgw} = z_{nn}^{0} + D_n^{\mathrm{T}}[-Z_0 D_{LGW} a_{LGW}^{-1} D_{LGW}^{\mathrm{T}} Z_0] D_n \quad (23)$$

$$a_{LGW} = M_{LGW}^{-1} + D_{LGW}^{\mathrm{T}} M_{LGW} D_{LGW} \quad (24)$$

It is worth noting that z_{nn}^{lgw} is nonlinear, which poses obstacle on SCC explicit formulation. It can be analyzed and linearized via neglecting the nondiagonal elements of $D_{LGW}^{\mathrm{T}} M_{LGW} D_{LGW}$, which will be discussed as follows. According to the differences of location vectors representing lines, units and wind farms in equations (18)-(22), switching off lines reflects both diagonal and nondiagonal elements of $D_{LGW}^{\mathrm{T}} M_{LGW} D_{LGW}$ in z_{nn}^{lgw}; while decommitting multiple units and wind farms only exert influence on the diagonal elements. So the physical meaning of nondiagonal element (i, j) in $D_{LGW}^{\mathrm{T}} M_{LGW} D_{LGW}$ is the mutual impedance between line l_i and l_j. Therefore, switching off multiple lines makes the value of nondiagonal element in $D_{LGW}^{\mathrm{T}} M_{LGW} D_{LGW}$ nonzero, that is matrix $D_{LGW}^{\mathrm{T}} M_{LGW} D_{LGW}$ is a full matrix. Hence, multiple lines switching makes a_{LGW} and z_{nn}^{lgw} be coupled and nonlinear.

In fact, the absolute values of diagonal elements in matrix a_{LGW} are much larger than non-diagonal ones [17]. Therefore, the non-diagonal elements in a_{LGW} can be ignored, and the inverse of a_{LGW} after linearization is derived as follows:

$$a_{LGW}^{-1} \approx \begin{bmatrix} a_L^{-1} & & \\ & a_G^{-1} & \\ & & a_W^{-1} \end{bmatrix} \quad (25)$$

$$a_L^{-1} = \mathrm{diag}[a_{l_1}^{-1}, \ldots, a_{l_{\mathrm{L}}}^{-1}] \quad (26)$$

$$a_G^{-1} = \mathrm{diag}[(-x_{g_1} + D_{g_1}^{\mathrm{T}} Z_0 D_{g_1})^{-1}, \ldots, (-x_{g_{\mathrm{G}}} + D_{g_{\mathrm{G}}}^{\mathrm{T}} Z_0 D_{g_{\mathrm{G}}})^{-1}] \quad (27)$$

$$a_W^{-1} = \mathrm{diag}[(-z_{w_1} + D_{w_1}^{\mathrm{T}} Z_0 D_{w_1})^{-1}, \ldots, (-z_{w_{\mathrm{W}}} + D_{w_{\mathrm{W}}}^{\mathrm{T}} Z_0 D_{w_{\mathrm{W}}})^{-1}] \quad (28)$$

Consequently, z_{nn}^{lgw} after linearization could be calculated as in (29). The nodal self-impedance in (29) considers

transmission lines switching, commitment of units and grid-connected wind farms. The SCC could be further obtained via equation (2). In addition, the error from linearization only comes from transmission switching [17].

$$z_{nn}^{lgw} \approx z_{nn}^{0} + \sum\nolimits_{l\in\Omega_{\mathrm{L}}} \mu_l \cdot \Delta z_{nn}^{l} + \sum\nolimits_{g\in\Omega_{\mathrm{G}}} \pi_g \cdot \Delta z_{nn}^{g} + \sum\nolimits_{w\in\Omega_{\mathrm{W}}} \lambda_w \cdot \Delta z_{nn}^{w} \quad (29)$$

IV. DAY-AHEAD SCHEDULING WITH SCC CONTRAINTS

A. OBJECTIVE FUNCTION

The proposed day-ahead scheduling model seeks to minimize the total cost consists of unit operation cost [31] and transmission switching cost, as shown in (30). The investment cost and generation cost of wind farms are not considered. Accordingly, the renewable power from wind farms could be adopted as much as possible because generation cost of wind farms is ignored.

$$\min \sum\nolimits_t \Big\{ \sum\nolimits_{g\in\Omega_{\mathrm{G}}} c_g \cdot \big[F_g(P_{g,t}) + SU_{g,t} + SD_{g,t}\big] + \sum\nolimits_{l\in\Omega_{\mathrm{L}}} c_l \cdot \mu_{l,t} \Big\} \quad (30)$$

B. SYSTEM OPERTATION CONSTRAINTS

The commitment constraints of units are formulated in (31)-(34). Constraints (31)-(32) calculate the startup/shutdown fuel consumption of thermal generating units. Constraints (33)-(34) represent minimum startup/shutdown time of units.

$$su_g \cdot (I_{g,t} - I_{g,(t-1)}) \le SU_{g,t}, 0 \le SU_{g,t} \quad (31)$$

$$sd_g \cdot (I_{g,(t-1)} - I_{g,t}) \le SD_{g,t}, 0 \le SD_{g,t} \quad (32)$$

$$(X_{g,(t-1)}^{\mathrm{on}} - T_g^{\mathrm{on}}) \cdot (I_{g,(t-1)} - I_{g,t}) \ge 0 \quad (33)$$

$$(X_{g,(t-1)}^{\mathrm{off}} - T_g^{\mathrm{off}}) \cdot (I_{g,t} - I_{g,(t-1)}) \ge 0 \quad (34)$$

In order to adopt the N-1 security requirement in the proposed model, binary variable s_l^c is introduced to represent the operation status of line l under contingency operation condition [22]. System operation constraints considering N-1 security requirement for all operation conditions are shown in (35)-(43). The limits of bus angle, units generation and wind farms generation [32] are shown in (35)-(37). Indeed, the uncertainty of wind generation are not included in the proposed day-ahead scheduling model, which can be incorporated by extending the proposed model into a stochastic or robust optimization framework. The uncertainty of wind generation could be incorporated by extending the proposed model into a stochastic [33], [34] or robust optimization framework [34]. The uncertainty handling method of wind generation will be the future research focus. The ramp up and down limits of thermal generating units are constrained in (38)-(39). Power balance of each bus is restricted in (40) [35]. The power flow capacity of each line is restricted in (41), the power flow of line l will be limited to 0 when $s_{l,t}^c = 1$ or $\mu_{l,t} = 1$. The Kirchhoff's laws are described in (42)-(43). Constraints (42)-(43) have to be satisfied if $s_{l,t}^c = 0$ and $\mu_{l,t} = 0$, while constraints (42)-(43) will be relaxed when $s_{l,t}^c = 1$ or $\mu_{l,t} = 1$ via the large number M, which also represents line l is not in service.

$$\theta^{\min} \le \theta_{n,t}^c \le \theta^{\max}, n \in \Omega_{\mathrm{N}}, c \in \Omega_{\mathrm{C}} \quad (35)$$

$$P_g^{\min} \cdot I_{g,t} \le P_{g,t}^c \le P_g^{\max} \cdot I_{g,t}, g \in \Omega_{\mathrm{G}}, c \in \Omega_{\mathrm{C}} \quad (36)$$

$$0 \le P_{w,t}^c \le P_{w,t}^f \cdot I_{w,t}, w \in \Omega_{\mathrm{W}}, c \in \Omega_{\mathrm{C}} \quad (37)$$

$$P_{g,t}^c - P_{g,(t-1)}^c \le UR_g \cdot I_{g,(t-1)} + P_g^{\min} \cdot (I_{g,t} - I_{g,(t-1)}) + P_g^{\max} \cdot (1 - I_{g,t}) \quad (38)$$

$$P_{g,(t-1)}^c - P_{g,t}^c \le DR_g \cdot I_{g,t} + P_g^{\min} \cdot (I_{g,(t-1)} - I_{g,t}) + P_g^{\max} \cdot (1 - I_{g,(t-1)}) \quad (39)$$

$$\sum\nolimits_{g\in\Omega_{(n)}} P_{g,t}^c + \sum\nolimits_{w\in\Omega_{(n)}} P_{w,t}^c - \sum\nolimits_{s(l)\in\Omega_{(n)}} P_{l,t}^c + \sum\nolimits_{r(l)\in\Omega_{(n)}} P_{l,t}^c = \sum\nolimits_{d\in\Omega_{(n)}} D_{d,t}, n \in \Omega_{\mathrm{N}}, c \in \Omega_{\mathrm{C}} \quad (40)$$

$$P_l^{\min}(1-\mu_{l,t})(1-s_{l,t}^c) \le P_{l,t}^c \le P_l^{\max}(1-\mu_{l,t})(1-s_{l,t}^c), \quad l \in \Omega_{\mathrm{L}}, c \in \Omega_{\mathrm{C}} \quad (41)$$

$$(\theta_{s(l),t} - \theta_{r(l),t}) \cdot y_l - P_{l,t}^c + M \cdot (1-\mu_{l,t})(1-s_{l,t}^c) \ge 0, \quad l \in \Omega_{\mathrm{L}}, c \in \Omega_{\mathrm{C}} \quad (42)$$

$$(\theta_{s(l),t} - \theta_{r(l),t}) \cdot y_l - P_{l,t}^c - M \cdot (1-\mu_{l,t})(1-s_{l,t}^c) \le 0, \quad l \in \Omega_{\mathrm{L}}, c \in \Omega_{\mathrm{C}} \quad (43)$$

Moreover, the relationship between commitment status of thermal generating units/ wind farms $I_{g,t}/I_{w,t}$ and operation variables $\pi_{g,t}/\lambda_{w,t}$ used in Section III to derive the SCC formulation are shown in (44)-(45).

$$I_{g,t} + \pi_{g,t} = 1 \quad (44)$$

$$I_{w,t} + \lambda_{w,t} = 1 \quad (45)$$

As discussed in Section III, the linearization error of SCC calculation is introduced from the transmission switching. Accordingly, the optimal solution obtained by the proposed model may not guarantee that the actual SCC level is below to the threshold value. A linearization error compensation approach in [17] is adopted here to ensure the solution accuracy, SCC constraints with the error compensation are shown in (46)-(48).

$$U_0/(z_{nn,t}^{lgw} + b_t^{\mathrm{B}} \cdot \Delta z_{nn,t}^{B}) \le I_n^{\mathrm{limit}}, n \in \Omega_{\mathrm{S}} \quad (46)$$

$$(1 - b_t^{\mathrm{B}}) + \mu_{l,t} \ge 1, l \in \Omega_t^{\mathrm{B}} \quad (47)$$

$$\sum\nolimits_{l\in\Omega_{\mathrm{B},t}} \mu_{l,t} \le N_t^{\mathrm{B}} - 1 + b_t^{\mathrm{B}} \quad (48)$$

where Ω_t^{B} is the set of lines which are selected to be switched off at hour t;b_t^{B} is a binary variable indicating the operation of lines in Ω_t^{B}; $\Delta z_{nn,t}^{\mathrm{B}}$ is the gap between the actual value of nodal self-impedance in (23) and the linearized value in (29); N_t^{B} is the total number of switched off lines in Ω_t^{B}.

The constrains in (46)-(48) are explained as follows. SCC constraint with error compensation is restricted in (46), where gap $\Delta z_{nn,t}^{\mathrm{B}}$ is used to compensate the linearization error. At first, $\Delta z_{nn,t}^{\mathrm{B}}$ is set to 0 to solve the model. Then SCC is calculated by (23). If the SCC level is below the threshold, the solution is optimal; otherwise, linearization error needs to be compensated. As a result, $\Delta z_{nn,t}^{\mathrm{B}}$ is calculated

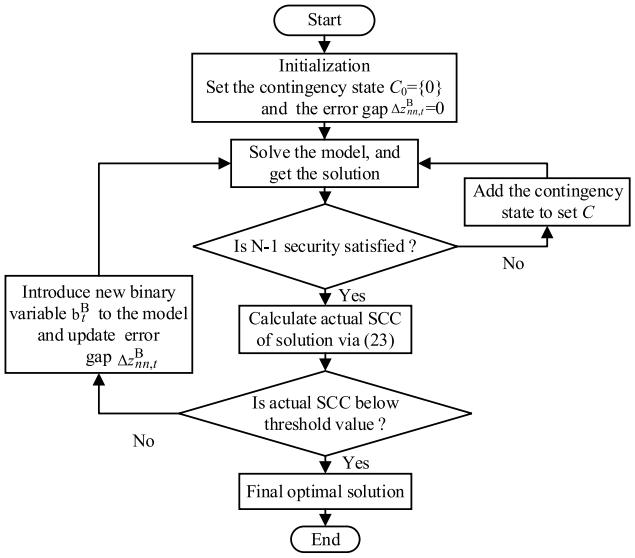

FIGURE 4. Flowchart of solving the proposed model.

via the actual and linearized value of nodal self-impedance. To embed $\Delta z^{B}_{nn,t}$ into the proposed day-ahead scheduling model, constraints (47)-(48) make sure that the lines are all switched off if and only if variable $b_{B,t}$ is equal to 1, and when $b_{B,t} = 1$ the gap $\Delta z^{B}_{nn,t}$ is added in (46) to compensate linearization error caused by the switched off lines in Ω^{B}_{t}.

C. SOLUTION PROCEDURE

The iterative algorithm with error compensation and N-1 security checking is shown in Fig. 4. The detailed procedure is as follows:

Step 1) Initialization. Set the contingency status to be $\Omega_C = \{0\}$ where only normal operation condition constraints are included. The error gap $\Delta z^{B}_{nn,t}$ is set to 0.

Step 2) Solve the proposed day-ahead scheduling model with SCC constraints and derive its optimal solution.

Step 3) Check the N-1 security of the solution. If the N-1 security cannot be satisfied, add the corresponding contingency status to set Ω_C and go back to Step 2; otherwise, go to Step 4.

Step 4) Calculate SCC level of the optimal solution via (23). If the SCC level is restricted below the threshold value, terminate the solution process with the final result; otherwise, introduce another binary variable shown in (47)-(48) to the model and obtain the new $\Delta z^{B}_{nn,t}$ to replace the previous one, go back to Step 2.

V. CASE STUDIES

The modified IEEE 30-bus system is used to verify the effectiveness and performance of the proposed day-ahead scheduling model, including two additional wind farms at bus 19 and 26 based on standard IEEE 30-bus system, and the wind

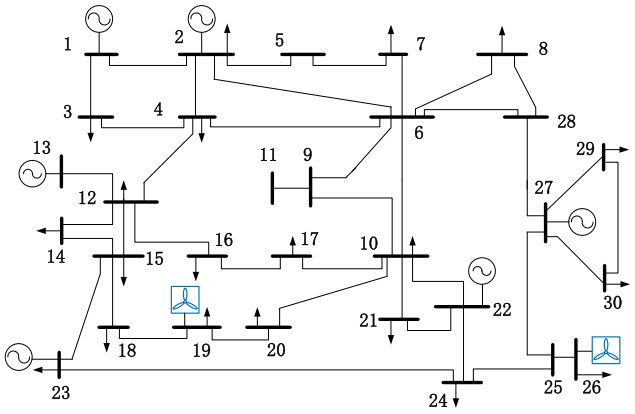

FIGURE 5. Modified IEEE 30-bus system with two wind farms.

farm locations are determined according to reference [36]. The topology of the modified IEEE 30-bus system is shown in Fig. 5. The capacities of thermal generating units and wind farms are 335MW and 80MW, respectively. Detailed data could be found in [37]. The subtransient reactance of thermal generating units ranges from 0.04p.u. to 0.055p.u., and the subtransient reactance of equivalent WTGs at bus 19 and 26 are 0.04 p.u. and 0.05 p.u., respectively. In addition, the maximum capacity of SCC level I_n^{limit} is set to be 12.5kA. The cost of switching off one transmission line c_l is set to be 100$, and the unit fuel cost is set as 5$/MBtu. GUROBI solver is used to solve the proposed MILP model.

A. ANALYSIS OF SCC WITH WIND FARMS INTEGRATION

In order to verify the impact of wind farms integration on the system SCC level, the SCC level of all buses with/without wind farms integration when all lines and units are in service are given in Fig. 6.

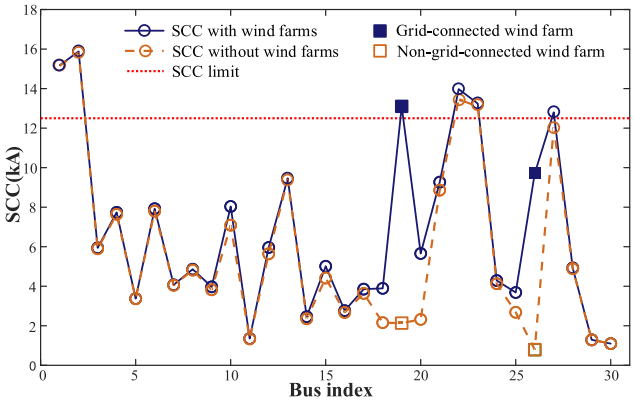

FIGURE 6. SCC level of all buses before and after wind farms integration.

As shown in Fig. 6, four buses (bus1, bus2, bus22, bus23) are with excessive SCC before wind farms integration, while SCC at bus 19 is drastically increased and SCC at bus 22, 23 and 27 are increased when the wind farms are integrated. The SCC level at bus 27 is larger than the I_n^{limit}. The SCC

level of bus 1 and 2 are merely impacted because of their long electrical distance to the wind farms. It can be concluded that wind farms integration increases the overall SCC level of the system, especially the SCC level of the buses located near the wind farms.

As can be observed from Fig. 6, six buses (bus1, bus2, bus19, bus22, bus23, bus27) are with excessive SCC level. The SCC constraints are added in the proposed day-ahead scheduling model at the aforementioned six buses. Four cases are used to demonstrate the advantages of the proposed day-ahead scheduling model as shown in Table 1, of which Case 4 represents the proposed model.

TABLE 1. The four cases with different settings.

Case	SCC constraints	SCC restrict methods		N-1 security
		Transmission switching	Commitment of units	
1	—	—	—	—
2	√	√	—	√
3	√	—	√	—
4	√	√	√	√

B. CASE STUDY OF SINGLE HOURS

Because electricity load level would affect the unit commitment results and consequently influence the system's SCC level, three different load levels with demand of 126MW, 200MW and 245MW are carried out to demonstrate the advantages of the proposed model. The three different load levels represent three typical hours in a day, which are 05:00, 14:00 and 21:00, respectively. The solution of Cases 1-4 at different hours are shown in Table 2.

TABLE 2. The results of cases 1-4 at different hours.

Hour	Case	In service units	Switched off lines	Excessive buses	Total cost($)
5	1	G_2,G_{22},W_{19},W_{26}	—	19,22	556.2
	2		$L_{15\text{-}18}$, $L_{10\text{-}22}$, $L_{22\text{-}24}$	—	877.9
	3		—	—	564.1
	4		—	—	564.1
14	1	G_1,G_2,G_{22}, W_{19},W_{26}	—	1,2,19,22	1157.4
	2		$L_{1\text{-}2}$, $L_{15\text{-}18}$, $L_{10\text{-}22}$, $L_{22\text{-}24}$	—	1557.4
	3	No feasible solution			
	4	G_1,G_2,W_{19},W_{26}	$L_{1\text{-}2}$	—	1270.8
21	1	G_1,G_2,G_{22}, G_{23},W_{19},W_{26}	—	1,2,19,22 23	1645.7
	2	No feasible solution			
	3	No feasible solution			
	4	G_1,G_2,G_{13},W_{19},W_{26}	$L_{1\text{-}2}$, $L_{15\text{-}18}$	—	1891.0

As shown in Table 2, the two wind farms are in service in all hours because wind farms do not incur any operation cost, which results in excessive SCC level at bus 19. The load level is in the valley at 5:00 and only two units are committed in Case 1. And the startup of thermal generating unit leads to excessive SCC level at bus 22. In Case 2, three transmission lines near the buses with excessive SCC level are switched off to reduce the system's SCC level with the highest cost among Cases 1-4. As can be observed from Case 3, the SCC level is reduced below the threshold via commitment of units. The costs of Case 3 and 4 are same, because the transmission switching process costs more and reducing the SCC level through commitment of units is cheaper.

The load is in a medium level at 14:00, where three units and two wind farms are committed, and the number of buses with excessive SCC increases to four. On the basis of unit commitment results in Case 1, four transmission lines are switched off to reduce the SCC level in Case 2. As compared to 5:00 in Case 2, more lines are switched off which might threaten the system security. Note that the model has no feasible solution in Case 3 at 14:00. Because higher load level needs more thermal generating units which could not essentially reduce the SCC level of all buses. When the unit commitment result meets the higher power demand, the SCC level could not be ensured at the same time.

From the solution of Case 4 at 14:00, the unit at bus 22 is shut down and one transmission line is switched off to reduce the SCC level. The units operation cost of Case 1 is 1157.4$, and the units operation cost of Case 4 is 1170.8$ which is quantified by the gap of total cost and transmission switching cost of line 1-2. As one can observe, units operation cost increases when units are decommitted to reduce SCC level in the proposed model. In addition, the total cost is less than that of Case 2 with switching off less lines. It can be concluded that the proposed model does well both in cost-effectiveness and N-1 security compared with merely using transmission switching in Case 2 and commitment of units in Case 3.

At 21:00, with the load level reached peak, unit at bus 23 starts up to supply the load which increases the number of buses with excessive SCC level to five. As a result, more lines have to be switched off, while the N-1 security requirement has to be simultaneously ensured. Particularly, Case 2 has no feasible solution because too many lines are switched off and the N-1 security criterion cannot be met.

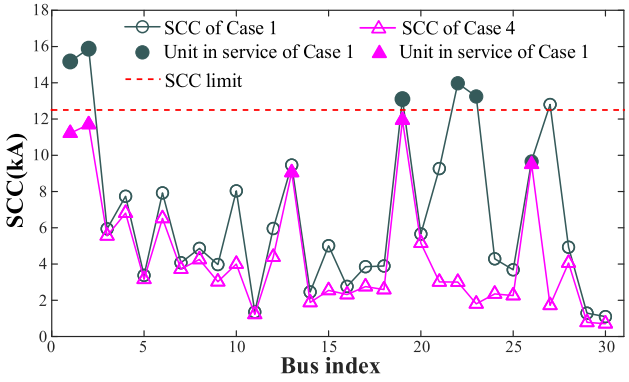

FIGURE 7. The SCC magnitude of cases 1 and 4 at 21:00.

To further illustrate the SCC restriction effectiveness of transmission switching and commitment of units in Case 4, the unit commitment results and the SCC level of Case 1 and 4 at 21:00 are shown in Fig. 7.

As shown in Fig. 7, the committed units and wind farms at bus 1, 2, 19, 22 and 23 lead to excessive SCC level in Case 1. In Case 4, units at bus 22 and 23 shut down which drastically reduces SCC level at the two buses. It further verifies the SCC restriction effectiveness of the commitment of units. Analyze the relation between switched-off lines and SCC excessive buses in Case 4, switched-off line 1-2 locates at SCC excessive bus 1 and 2, another switched-off line 15-18 is adjacent to excessive bus 19. These two switched-off lines 1-2 and 15-18 both locate near SCC excessive buses 1, 2 and 19. Switching off lines near SCC excessive bus can effectively reduce the SCC level.

In conclusion, the proposed day-ahead scheduling model performs better in cost-effectiveness, while also guarantees system N-1 security by avoiding switching off too many lines.

C. CASE STUDY OF DAY-AHEAD SCHEDULING

To verify the effectiveness of the proposed model from the point of day-ahead scheduling, Case 4 is applied in a day-ahead scheduling model compared to the results of Case 1. The load curve, number of buses with excessive SCC level and unit commitment results of Case 1 are plotted in Fig. 8.

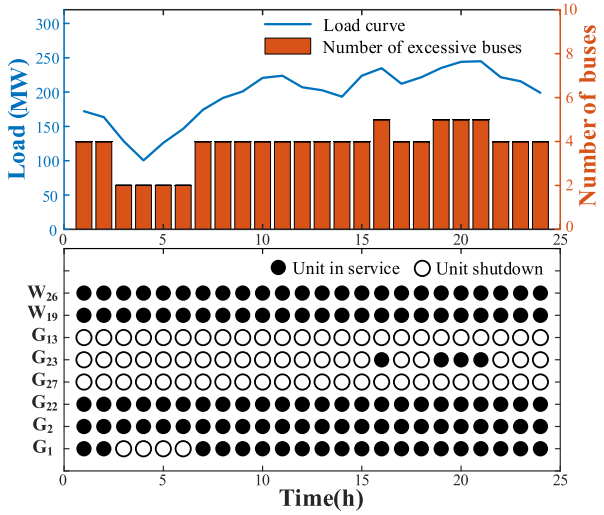

FIGURE 8. Load curve, number of buses with excessive SCC and unit commitment results of case 1.

As shown in Fig. 8, the number of committed units changes as the load curve changes during the day, which also directly influences the SCC level. The number of buses with excessive SCC level increases as the electricity load increases. To restrict the SCC level, the proposed model is used to derive a day-ahead scheduling result to limit system's SCC magnitude. The switched-off lines in Case 4 are shown in Table 3. The unit commitment result and number of switched-off lines of Case 4 are shown in Fig. 9.

As shown in Fig. 9 and Table 3, two wind farms are both in service in case 4 compared to the unit commitment results in Case 1. In Fig. 9, the unit at bus 22 is OFF because of its high subtransient reactance. In hours 1:00-2:00, two

TABLE 3. The switched-off lines of case 4.

Hour	Switched-off lines
1-2	$L_{1\text{-}2}$
3-5	—
6-9	$L_{1\text{-}2}$
10-11	$L_{1\text{-}2}$, $L_{15\text{-}18}$
12-14	$L_{1\text{-}2}$
15-19	$L_{1\text{-}2}$, $L_{15\text{-}18}$
20-22	$L_{1\text{-}2}$, $L_{15\text{-}18}$
23	$L_{1\text{-}2}$, $L_{2\text{-}6}$
24	$L_{1\text{-}2}$

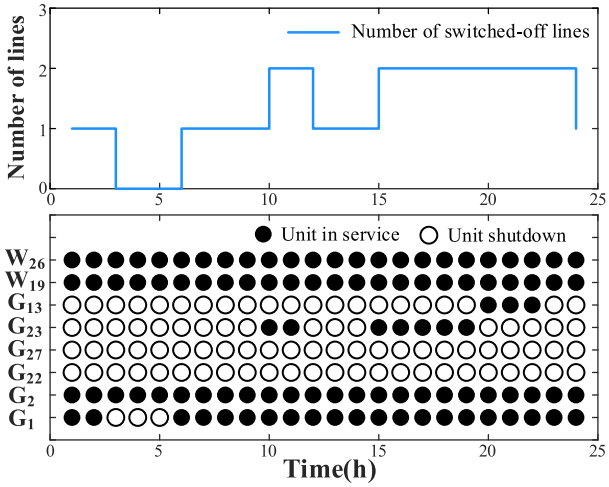

FIGURE 9. Number of switched-off lines and unit commitment of case 4.

thermal generating units are in service to satisfy the load curve, and line 1-2 is switched off to reduce the SCC level. The generating unit at bus 1 shuts down and no lines are switched off in 3:00-5:00 because the commitment of units could independently reduce SCC level when load is at a lower level. As the load level increases in the daytime, two generating units starts up and line 1-2 is switched off to restrict the SCC level at 6:00-9:00 and 12:00-14:00, respectively. In hours 10:00-11:00 and 15:00-19:00, unit at bus 23 starts up and line 15-18 is switched off as more generating units start up to satisfy the increased load. Note that in Case 4, unit at bus 13 starts up in hours 20:00-22:00 instead of unit at bus 23 because the load level is at the peak in the daytime and the total generation after unit at bus 13 starts up cannot satisfy the increased load, and unit at bus 13 is still in service at 22:00 because of its minimum shut time limit. And at this time, the line 1-2 and line 12-18 are still switched off to reduce the SCC level. Finally, the load falls back to normal level in hours 23:00-24:00, and the number of committed units decreases. It is worth noting that the unit commitment is same at hours 23:00 and 24:00, while the number of switched-off lines is different. Line 1-2 and line 2-6 are switched off at hour 23:00, while only line 1-2 is switched off at hour 24:00. The reason is that line 2-6 is switched off to relive the transmission congestion at 23:00 [38], [39]. Therefore, it could be concluded that the proposed model provides an economic and secure day-ahead scheduling solution while ensures the system SCC level within a permissible level.

VI. CONCLUSION

This paper proposes a day-ahead scheduling model with SCC constraints while considering integration of wind farms, transmission switching and commitment of units. Grid-connected wind farms are converted to equivalent single-machine WTG to participate in the SCC formulation. Moreover, the N-1 security requirement is considered to ensure the system reliability.

The case studies also show the following observations: 1) SCC could be effectively restricted via the proposed model with transmission switching and commitment of units while considering grid-connected wind farms; 2) decommitting units could reduce SCC level, which has better performance when combined with transmission switching; 3) the model proposed in this paper has less impact on system security with switching off less lines; 4) the proposed model performs better in cost-effectiveness while satisfying the N-1 security requirement.

ACKNOWLEDGMENT

This work was supported by Sichuan Science and Technology Program under Grant 2021YFH0029.

REFERENCES

[1] D. Wu, G. Li, M. Javadi, A. M. Malyscheff, M. Hong, and J. N. Jiang, "Assessing impact of renewable energy integration on system strength using site-dependent short circuit ratio," *IEEE Trans. Sustain. Energy*, vol. 9, no. 3, pp. 1072–1080, Jul. 2018.

[2] F. R. Badal, P. Das, S. K. Sarker, and S. K. Das, "A survey on control issues in renewable energy integration and microgrid," *Protection Control Mod. Power Syst.*, vol. 4, no. 1, pp. 1–27, Dec. 2019.

[3] J. G. Rolim and L. J. B. Machado, "A study of the use of corrective switching in transmission systems," *IEEE Trans. Power Syst.*, vol. 14, no. 1, pp. 336–341, Feb. 1999.

[4] M. Abdi-Khorsand, M. Sahraei-Ardakani, and Y. M. Al-Abdullah, "Corrective transmission switching for N-1-1 contingency analysis," *IEEE Trans. Power Syst.*, vol. 32, no. 2, pp. 1606–1615, Mar. 2017.

[5] M. Erdiwansyah, H. Husin, M. Z. Nasaruddin, and A. Muhibbuddin, "A critical review of the integration of renewable energy sources with various technologies," *Protection Control Mod. Power Syst.*, vol. 6, no. 1, pp. 1–18, Dec. 2021.

[6] Y. Zhou, L. Zhao, and W.-J. Lee, "Robustness analysis of dynamic equivalent model of DFIG wind farm for stability study," *IEEE Trans. Ind. Appl.*, vol. 54, no. 6, pp. 5682–5690, Nov./Dec. 2018.

[7] P.-H. Huang, M. E. Moursi, W. Xiao, and J. Kirtley, "Subsynchronous resonance mitigation for series-compensated DFIG-based wind farm by using two-degree-of-freedom control strategy," *IEEE Trans. Power Syst.*, vol. 30, no. 3, pp. 1442–1454, May 2015.

[8] J. Brochu, C. Larose, and R. Gagnon, "Generic equivalent collector system parameters for large wind power plants," *IEEE Trans. Energy Convers.*, vol. 26, no. 2, pp. 542–549, Jun. 2011.

[9] J. Zou, C. Peng, H. Xu, and Y. Yan, "A fuzzy clustering algorithm-based dynamic equivalent modeling method for wind farm with DFIG," *IEEE Trans. Energy Convers.*, vol. 30, no. 4, pp. 1329–1337, Dec. 2015.

[10] X. Wang, H. Yu, Y. Lin, Z. Zhang, and X. Gong, "Dynamic equivalent modeling for wind farms with DFIGs using the artificial bee colony with K-means algorithm," *IEEE Access*, vol. 8, pp. 173723–173731, 2020.

[11] Y. Zhou, L. Zhao, I. B. M. Matsuo, and W.-J. Lee, "A dynamic weighted aggregation equivalent modeling approach for the DFIG wind farm considering the Weibull distribution for fault analysis," *IEEE Trans. Ind. Appl.*, vol. 55, no. 6, pp. 5514–5523, Nov. 2019.

[12] S. Huang, Q. Wu, L. Cheng, and Z. Liu, "Optimal reconfiguration-based dynamic tariff for congestion management and line loss reduction in distribution networks," *IEEE Trans. Smart Grid*, vol. 7, no. 3, pp. 1295–1303, May 2016.

[13] E. B. Fisher, R. P. O'Neill, and M. C. Ferris, "Optimal transmission switching," *IEEE Trans. Power Syst.*, vol. 23, no. 3, pp. 1346–1355, Aug. 2008.

[14] M. Soroush and J. D. Fuller, "Accuracies of optimal transmission switching heuristics based on DCOPF and ACOPF," *IEEE Trans. Power Syst.*, vol. 29, no. 2, pp. 924–932, Mar. 2014.

[15] T. Han, Y. Song, and D. J. Hill, "Ensuring network connectedness in optimal transmission switching problems," *IEEE Trans. Circuits Syst. II, Exp. Briefs*, vol. 68, no. 7, pp. 2603–2607, Jul. 2021.

[16] S. R. Salkuti, "Congestion management using optimal transmission switching," *IEEE Syst. J.*, vol. 12, no. 4, pp. 3555–3564, Dec. 2018.

[17] Z. Yang, H. Zhong, Q. Xia, and C. Kang, "Optimal transmission switching with short-circuit current limitation constraints," *IEEE Trans. Power Syst.*, vol. 31, no. 2, pp. 1278–1288, Mar. 2016.

[18] K. W. Hedman, R. P. O'Neill, E. B. Fisher, and S. S. Oren, "Optimal transmission switching—Sensitivity analysis and extensions," *IEEE Trans. Power Syst.*, vol. 23, no. 3, pp. 1469–1479, Aug. 2008.

[19] C. Liu, J. Wang, and J. Ostrowski, "Static switching security in multiperiod transmission switching," *IEEE Trans. Power Syst.*, vol. 27, no. 4, pp. 1850–1858, Nov. 2012.

[20] P. Henneaux and D. S. Kirschen, "Probabilistic security analysis of optimal transmission switching," *IEEE Trans. Power Syst.*, vol. 31, no. 1, pp. 508–517, Jan. 2016.

[21] A. Khodaei and M. Shahidehpour, "Transmission switching in security-constrained unit commitment," *IEEE Trans. Power Syst.*, vol. 25, no. 4, pp. 1937–1945, Nov. 2010.

[22] K. W. Hedman, M. C. Ferris, R. P. O'Neill, E. B. Fisher, and S. S. Oren, "Co-optimization of generation unit commitment and transmission switching with N-1 reliability," *IEEE Trans. Power Syst.*, vol. 25, no. 2, pp. 1052–1063, May 2010.

[23] R. Saavedra, A. Street, and J. M. Arroyo, "Day-ahead contingency-constrained unit commitment with co-optimized post-contingency transmission switching," *IEEE Trans. Power Syst.*, vol. 35, no. 6, pp. 4408–4420, Nov. 2020.

[24] J. Shi and S. S. Oren, "Stochastic unit commitment with topology control recourse for power systems with large-scale renewable integration," *IEEE Trans. Power Syst.*, vol. 33, no. 3, pp. 3315–3324, May 2018.

[25] J. Lin, Y. Hou, G. Zhu, S. Luo, P. Li, L. Qi, and L. Wang, "Co-optimization of unit commitment and transmission switching with short-circuit current constraints," *Int. J. Electr. Power Energy Syst.*, vol. 110, pp. 309–317, Sep. 2019.

[26] W. Li, P. Chao, X. Liang, D. Xu, and X. Jin, "An improved single-machine equivalent method of wind power plants by calibrating power recovery behaviors," *IEEE Trans. Power Syst.*, vol. 33, no. 4, pp. 4371–4381, Jul. 2018.

[27] R. Fang, R. Shang, M. Wu, C. Peng, and X. Guo, "Application of gray relational analysis to k-means clustering for dynamic equivalent modeling of wind farm," *Int. J. Hydrogen Energy*, vol. 42, pp. 20154–20163, Aug. 2017.

[28] *IEEE Application Guide for Capacitance Current Switching for AC High-Voltage Circuit Breakers Rated on a Symmetrical Current Basis*, Standard ANSI/IEEE C37.012-1979, Feb. 1979, pp. 1–54.

[29] J. J. Grainger and W. D. Stevenson, *Power System Analysis*. New York, NY, USA: McGraw-Hill, 1994.

[30] D. J. Tylavsky and G. R. L. Sohie, "Generalization of the matrix inversion lemma," *Proc. IEEE*, vol. 74, no. 7, pp. 1050–1052, Jul. 1986.

[31] S. S. Reddy and J. A. Momoh, "Minimum emission dispatch in an integrated thermal and wind energy conservation system using self-adaptive differential evolution," in *Proc. IEEE PES PowerAfrica*, Jun. 2016, pp. 269–273.

[32] S. S. Reddy, "Optimal scheduling of thermal-wind-solar power system with storage," *Renew. Energy*, vol. 101, pp. 1357–1368, Feb. 2017.

[33] Y. Zhang, J. Wang, B. Zeng, and Z. Hu, "Chance-constrained two-stage unit commitment under uncertain load and wind power output using bilinear benders decomposition," *IEEE Trans. Power Syst.*, vol. 32, no. 5, pp. 3637–3647, Sep. 2017.

[34] C. He, L. Wu, T. Liu, and M. Shahidehpour, "Robust co-optimization scheduling of electricity and natural gas systems via ADMM," *IEEE Trans. Sustain. Energy*, vol. 8, no. 2, pp. 658–670, Apr. 2017.

[35] S. S. Reddy, "Optimization of railroad electrical systems with the integrated smart grid," *Int. J. Appl. Eng. Res.*, vol. 12, pp. 1027–1030, Nov. 2017.

[36] X. Li, X. Zhang, L. Wu, P. Lu, and S. Zhang, "Transmission line overload risk assessment for power systems with wind and load-power generation correlation," *IEEE Trans. Smart Grid*, vol. 6, no. 3, pp. 1233–1242, May 2015.
[37] C. P. Prajapati and A. K. Dahiya, "Performance improvement of IEEE-30 bus system using UPFC and TCSC on PSAT," in *Proc. IEEE Students Conf. Eng. Syst. (SCES)*, Allahabad, India, May 2019, pp. 1–6.
[38] M. Khanabadi, H. Ghasemi, and M. Doostizadeh, "Optimal transmission switching considering voltage security and N-1 contingency analysis," *IEEE Trans. Power Syst.*, vol. 28, no. 1, pp. 542–550, Feb. 2013.
[39] M. Khanabadi, Y. Fu, and C. Liu, "Decentralized transmission line switching for congestion management of interconnected power systems," *IEEE Trans. Power Syst.*, vol. 33, no. 6, pp. 5902–5912, Nov. 2018.

HAOCHENG HUA received the B.S. degree in electrical engineering from Sichuan University, Chengdu, China, in 2019, where he is currently pursuing the M.S. degree. His research interests include optimal operation of power grids and short-circuit current restriction.

TIANQI LIU (Senior Member, IEEE) received the B.S. and M.S. degrees in electrical engineering from Sichuan University, Chengdu, China, in 1982 and 1986, respectively, and the Ph.D. degree in electrical engineering from Chongqing University, Chongqing, China, in 1996. She is currently a Professor with the College of Electrical Engineering, Sichuan University. Her main research interests include power system analysis and stability control, HVDC, optimal operation, dynamic security analysis, dynamic state estimation, and load forecast.

CHUAN HE (Member, IEEE) received the B.S., M.S., and Ph.D. degrees in electrical engineering from Sichuan University, Chengdu, China, in 2011, 2014, and 2018, respectively. He was a Visiting Ph.D. Student at Clarkson University, Potsdam, NY, USA, from 2015 to 2017. He is currently an Associate Research Professor with the College of Electrical Engineering, Sichuan University. His research interests include robust optimization on power system operation and planning with renewable energy.

LU NAN (Member, IEEE) received the B.S. and Ph.D. degrees in electrical engineering from Sichuan University, Chengdu, China, in 2016 and 2020, respectively. She was a Visiting Ph.D. Student at Stevens Institute of Technology, Hoboken, USA, from 2018 to 2019. She is currently a Research Associate with the College of Electrical Engineering, Sichuan University. Her research interests include vulnerability analysis and optimal operation of power grids.

HONG ZENG received the M.S. degree in electrical engineering from Sichuan University, Chengdu, China, in 2019. She is currently an Assistant Engineer with Tianfu Power Supply Company, State Grid Sichuan Electrical Power Company. Her research interests include power grid planning and renewable generation.

XIAOTONG HU received the Ph.D. degree in electrical engineering from Sichuan University, Chengdu, China, in 2019. He is currently a Senior Engineer with State Grid Sichuan Electrical Power Company. His research interests include power generation control and renewable generation.

BIN CHE received the B.S. degree in engineering from Sichuan University, China, in 2008, the M.S. degree in engineering from the University of Nottingham, U.K., in 2009, and the Ph.D. degree in engineering from Cardiff University, U.K., in 2013. He is currently a Senior Engineer with Economics and Technology Research Institute, State Grid Ningxia Electric Power Company. His research interest includes power grid planning.